Inorganic Chemistry

Article

pubs.acs.org/IC

Implications of Stoichiometry-Controlled Structural Changeover Between Heteroleptic Trigonal $[Cu(phenAr_2)(py)]^+$ and Tetragonal $[Cu(phenAr_2)(py)_2]^+$ Motifs for Solution and Solid-State Supramolecular Self-Assembly

Subhadip Neogi,*[,‡] Gregor Schnakenburg,[§] Yvonne Lorenz,[§] Marianne Engeser,[§] and Michael Schmittel*[,‡]

[‡]Center of Micro and Nanochemistry and Engineering, Organische Chemie I, Universität Siegen, Adolf-Reichwein-Strasse 2, D-57068 Siegen, Germany

[§]Fachgruppe Chemie der Universität Bonn, Gerhard-Domagk-Strasse 1, 53121 Bonn, Germany

Supporting Information

ABSTRACT: A stoichiometric variant of the HETPYP concept (HETeroleptic PYridine and Phenanthroline metal complexes) opens the venue to heteroleptic metallosupramolecular HETPYP-I assemblies both in solution and the solid state, involving the trigonal $[Cu(phenAr_2)(py)]^+$ coordination motif ($phenAr_2$ = 2,9-diarylphenanthroline; py = various oligopyridines). Combining the same building blocks at another stoichiometric ratio furnished metallosupramolecular HETPYP-II aggregates in the solid state, now based on the tetrahedral $[Cu(phenAr_2)(py)_2]^+$ coordination motif. Thus, a stoichiometry-controlled structural changeover based on the relative amounts of oligopyridines leads from a discrete assembly with trigonally coordinated copper(I) centers to a coordination polymer with tetrahedrally coordinated copper(I) ions, as shown by solid state studies. In solution, the analysis of both stoichiometric variants indicates that the HETPYP-I structure is congruent with that in the solid state, while the HETPYP-II assembly, as established through DOSY NMR and dynamic light scattering measurements, is only oligomeric at low temperature. At room temperature, i.e. due to entropic costs, the latter assembly prefers to keep "unsaturated" coordination sites that are in rapid exchange, making it an interesting system as a dynamic protecting group and for constitutional dynamic materials through the exchange and reshuffling of components.

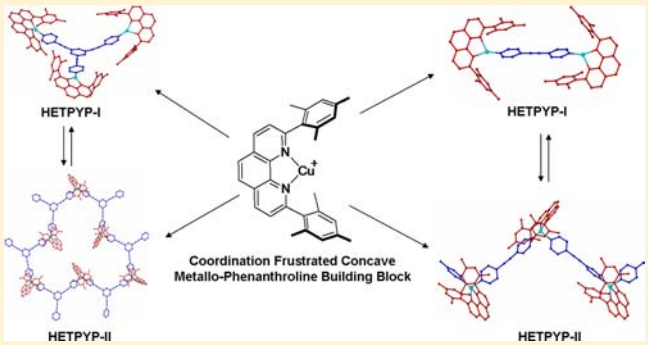

INTRODUCTION

Over the past two decades, metallosupramolecular chemistry has witnessed forceful research activities to unravel the mysteries of self-assembly furnishing well-defined, discrete architectures under thermodynamic control from a collection of two, three, or even more components.[1] On one side, current research aims at developing huge highly symmetric supramolecular entities, such as virus analogs,[2] making multiple use of a single component (in combination with metal ions as a glue), while on the other side intricate self-sorting protocols are searched to build more and more geometrically irregular multicomponent aggregates.[3] Interest in the latter[4] emerges not only because of academic fascination with intricate structures, but also due to possible emergent properties of multicomponent aggregates, a feature well-known in biological systems.[5] The increased complexity, however, goes along with an augmented number of possible reaction products and thus raises the question, how to control the formation of a single discrete supramolecule in a fully dynamic setting with more and more components being available.[6] Unsurprisingly, the successful self-assembly of multiple components into discrete heteroleptic structures is still much less documented.[3,7] Herein, we will present not only a new three-component self-assembly system, but also its use in reversible structural changeovers, simply controlled by the stoichiometric ratio of the components. Such protocols may open the perspective to switching emergent properties of multicomponent systems through the deliberate addition and removal of components.

At present, additive-triggered structural changeovers in supramolecular systems are hardly known.[8] Hupp and Nguyen elaborated a loop to square conversion by rigidifying the bridging ligand through addition of Zn^{2+} to a salene binding site.[9] Utilizing the reaction of an alkyne with $Co_2(CO)_8$ for supramolecule-to-supramolecule transformations, Stang and coworkers developed the conversion of a [6 + 6] hexagon to two

Received: June 18, 2012
Published: September 26, 2012

   dx.doi.org/10.1021/ic301286w | *Inorg. Chem.* 2012, 51, 10832−10841

Scheme 1. Three Different Possibilities of Heteroleptic Complexation in the HETPYP Concept

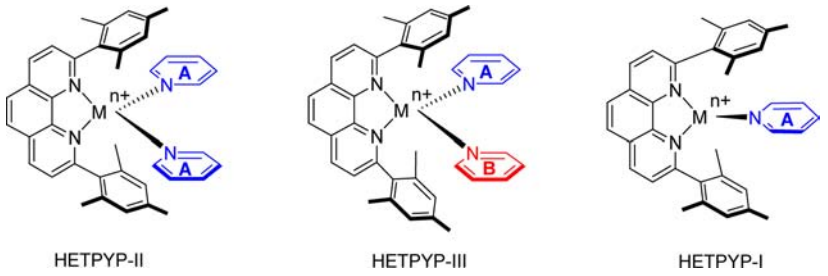

Scheme 2. Ligands Used in the Present Study (With Atom Numbering Scheme)

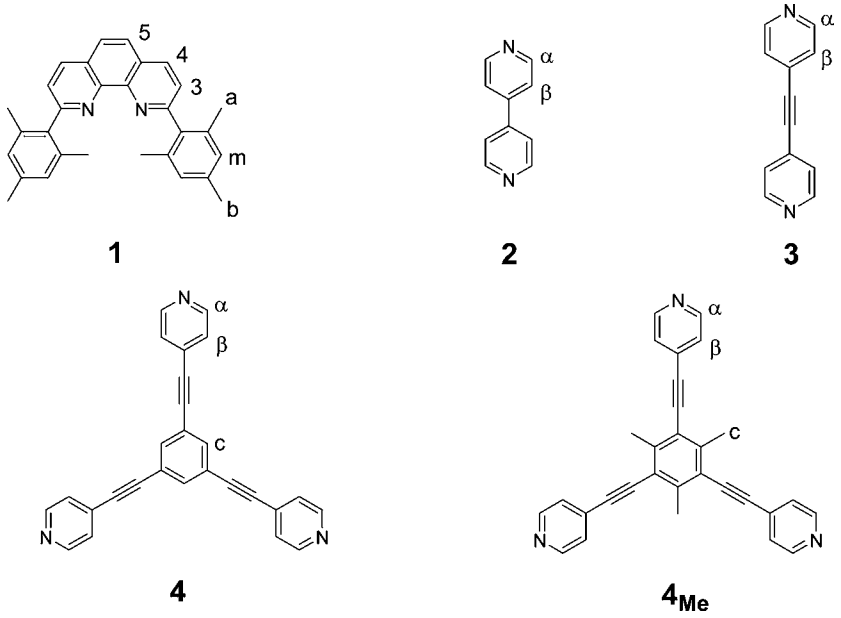

[3 + 3] hexagons and of a triangle-square mixture to [2 + 2] rhomboids.[10] Reversible interconversion of a metallosupramolecular triangle and a coordination polymer was effected by changing the solvent that acts as an axial ligand on the bridging copper ions, as described by Mirkin.[8b] Obviously, such transformations should not mistaken for supramolecular isomerism.[11,12]

For setting up stoichiometry-responsive multicomponent systems and their structural conversions, we envisaged to use a heteroleptic complexation unit that is both tolerant to different lengths/angles of the ligands and to different coordination angles/scenarios at the metal site. As possible coordination units for such transformations, one may identify end-capped square-planar palladium and platinum units as these cornerstones allow for combinations with a variety of ligands, such as pyridines, alkynes, carboxylates, and nitriles, leading to exciting heteroleptic metallosupramolecular structures.[13,14] A similarly attractive cornerstone is the complex $[M(phenAr_2)]^+$ with its sterically shielded 2,9-diarylphenanthroline ($phenAr_2$), because in our earlier work it has proven itself as a versatile building unit for a large number of supramolecular heteroleptic aggregates.[15−19] Notably, the $[M(phenAr_2)]^+$ unit cannot combine with a second $phenAr_2$. Thus, the system remains in a coordinatively frustrated situation until it coordinates to a second slim ligand L (L: pyridine (py),[15,16a] phenanthroline,[17,18] or terpyridine[19]) to fill the vacant site(s) by generating the complex $[M(phenAr_2)(L)]^+$.

For inducing structural alterations through addition of components, the highly dynamic coordination motif $[M(phenAr_2)(py)]^+$ seemed most promising to us. Unlike L = phenanthroline or terpyridine,[20] the nonchelate ligand pyridine provides a much weaker binding to the metal ion thus offering an increased dynamics.[21] On the basis of these considerations, we recently developed the HETPYP (heteroleptic pyridine and phenanthroline metal complexes) concept,[15] in which the central copper(I) ion sets up a tetrahedral coordination scenario with one phenanthroline and two pyridine ligands. In our quest to control supramolecular structures by stoichiometry, we envisioned that the HETPYP approach may be ideal by virtue of various Cu^+−N(py) bonding settings. To our perception, three different possibilities may arise in HETPYP assemblies (see Scheme 1): (a) a HETPYP-II coordination as reported previously by us,[15,16b] (b) a trisheteroleptic complex (HETPYP-III) arising from a $[M(phenAr_2)]^+$ unit and two dissimilar pyridine ligands (similar to the end-capped Pt^{2+} or Pd^{2+} metal ions reported by Fujita and co-workers),[22] and (c) formation of a new tricoordinated[23] HETPYP-I type complex, in which a single pyridine ligand is attached to the frustrated $[M(phenAr_2)]^+$ center.

Herein, we describe how one can set up (i) trigonally coordinated copper(I) centers (HETPYP-I) as novel building blocks for discrete supramolecular assemblies and (ii) a stoichiometry-dependent changeover between discrete $[Cu(phenAr_2)(py)]^+$ assemblies (HETPYP-I) and coordination polymers in the solid state, the latter based on tetrahedral

dx.doi.org/10.1021/ic301286w | Inorg. Chem. 2012, 51, 10832−10841

Table 1. Summary of Crystallographic Data for C1$^{(I)}$, C1$^{(II)}$, C2, C3$^{(II)}$, and C4$^{(I)}$

	C1$^{(I)}$	C1$^{(II)}$	C2	C3$^{(II)}$	C4$^{(I)}$
formula	$C_{84}H_{72}Cl_4Cu_2F_{12}N_6P_2$	$C_{42}H_{36}CuF_6N_4P$	$C_{76}H_{68}Cu_2F_6N_6O_6S_2Cl_4$	$C_{80}H_{72}Cu_2F_6N_8P$	$C_{122}H_{111}Cl_2Cu_3F_{18}N_9OP_3$
fw	1724.30	805.26	1608.36	1417.51	2415.63
cryst syst	triclinic	orthorhombic	triclinic	monoclinic	monoclinic
space group	$P\bar{1}$	$Pna2_1$	$P\bar{1}$	$P2_1/n$	$C2/c$
a (Å)	0.861(10)	18.924(4)	11.204(15)	14.548(7)	41.081(3)
b (Å)	12.328(12)	10.675(3)	12.427(16)	36.735(17)	23.644(16)
c (Å)	14.657(15)	18.521(5)	13.711(16)	16.967(8)	27.532(18)
α	91.22(4)		94.47(4)		
β (deg)	103.27(3)		102.37(4)	95.55(10)	117.06(3)
γ	95.78(3)		101.74(4)		
V (Å^3)	1898.3(3)	3741.41(17)	1810.7(4)	9025.3(7)	23814(3)
Z	1	4	1	4	8
D_{calcd} (g cm^{-3})	1.508	1.430	1.475	1.043	1.348
μ (mm^{-1})	0.824	0.693	0.866	0.541	0.697
$F(000)$	882	1656	826	2940	9936
T (min.)	0.673	0.706	0.846	0.909	0.756
T (max.)	0.952	0.934	0.950	0.938	0.959
GOF on F^2	1.045	1.045	1.026	0.917	1.221
R_1 [$I > 2\sigma(I)$]	0.0322	0.0458	0.0748	0.1178	0.1091
R_2 [$I > 2\sigma(I)$]	0.0834	0.1211	0.1719	0.2317	0.3108

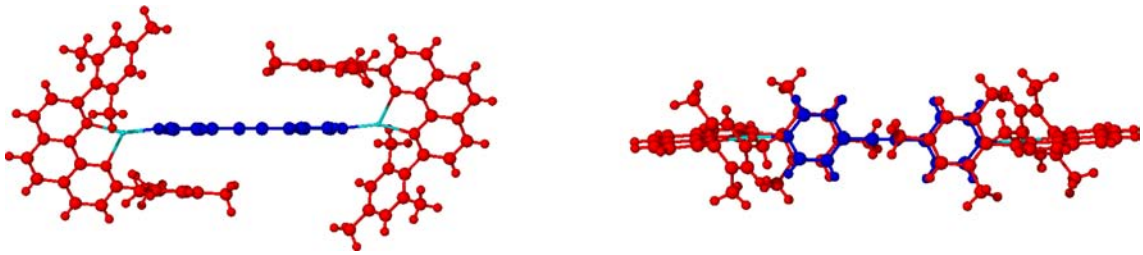

Figure 1. Side view (left) and top view (right) of the crystal structure for complex **C1**$^{(I)}$.

$[Cu(phenAr_2)(py)_2]^+$ complexes (HETPYP-II). The origin of the change is based solely on the reversible attachment of one versus two pyridine ligands at the frustrated $[Cu(phenAr_2)]^+$ site (Scheme 1). In solution, on the basis of 1D and 2D NMR, DOSY NMR, ESI-FTICR mass spectrometry, and dynamic light scattering (DLS) data, we see the same structural changeover.

RESULTS AND DISCUSSION

All ligands used in this study are depicted in Scheme 2. 4,4′-Bipyridine (**2**) is commercially available, while ligands **1**, **3**, and **4** were prepared according to literature procedures.[24] For convenience, HETPYP-I and HETPYP-II complexes based on identical ligands are denoted as **Cn**$^{(I)}$ and **Cn**$^{(II)}$, respectively.

Solid State Studies. *Self-Assembly of Bipyridine* ***3*** *and* $[Cu(1)]^+$ *(Complexes* ***C1****$^{(I)}$,* ***C1****$^{(II)}$, and* ***C2****).* As a starting point to elaborate HETPYP-I vs HETPYP-II self-assembly, we decided to evaluate the heteroleptic complexation scenario of **1**, **3**, and $[Cu(MeCN)_4]PF_6$. Because pyridines typically form homoleptic complexes in the presence of many metal ions,[25] it seemed reasonable to avoid formation of any unwanted homoleptic complex right at the onset by combining all components sequentially. Keeping this in mind, **1** was first fed with one equivalent of Cu^+ in dichloromethane-d_2 to form the capped and coordinatively frustrated metal monoligand complex $[Cu(\mathbf{1})]^+$. After mixing ligand **3** with $[Cu(\mathbf{1})]^+$ in a 1:2 ratio, the color of the solution immediately turned from yellow to orange. Heteroleptic complexation along the HETPYP-I design was proven by X-ray diffraction analysis. Orange-colored single crystals, suitable for the X-ray study, were grown by slow diffusion of diethyl ether into a dichlorobenzene solution of **C1**$^{(I)}$. The compound crystallizes in the triclinic space group $P\bar{1}$ (Table 1) with the asymmetric unit consisting of one copper(I) ion, ligand **1**, one-half of ligand **3**, a PF_6^- anion, and a 1,2-dichlorobenzene solvent molecule. The copper(I) ion is linked unsymmetrically to the two nitrogens of the phenanthroline (2.10 Å and 1.98 Å) and one pyridine nitrogen (1.90 Å) thus accepting only three dative coordination bonds (Figure 1). The PF_6^- anion is situated on one side of the $[Cu(\mathbf{1})]^+$ motif exhibiting only negligible interaction with the copper(I) ion (3.25 Å).[26] While the trigonal copper(I) motif is rare, it has been documented previously with various ligands in mononuclear complexes[23,27] and within an oligonuclear oligopyridine helicate with all L–Cu–L angles at ∼120°.[28]

The less-commonly Y-shaped geometry (one angle compressed from 120°, the other two expanded), as observed herein, occurs only when a chelating ligand forces one of the angles to be narrower than the expected 120° trigonal planar geometry.[27] Each ligand **3** connects two copper(I) phenanthroline units (Figure 1) to form a discrete dumbbell-shaped structure with a Cu···Cu separation of 13.45 Å, with the planes of phenanthroline and pyridine rings being perpendicular to each other. One of the mesityl groups of **1** is found to be slanted somewhat toward the bipyridine plane (Figure 1, side view) thus experiencing strong π-stacking interactions with the

dx.doi.org/10.1021/ic301286w | Inorg. Chem. 2012, 51, 10832–10841

pyridine ring (3.59 Å). Another strong π-stacking interaction is observed between the pyridine ring and the dichlorobenzene solvent molecule (3.80 Å). These strong secondary interactions appear to stabilize the overall structure. The overall two-dimensional (2D) packing diagram with its one-dimensional channel structure is depicted in Figure 2. The channels are filled with solvent molecules and PF_6^- anions.

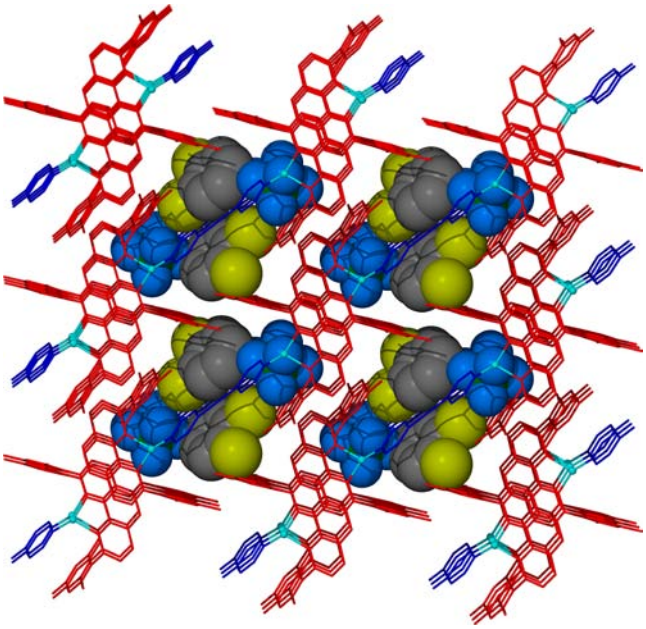

Figure 2. Two dimensional packing diagram of $\mathbf{C1}^{(I)}$ along the crystallographic *a* axis, showing 1,2-dichlorobenzene solvent molecules and PF_6^- anions embedded inside the one-dimensional channels. Color code: **1**, red; **3**, blue; copper, cyan.

Changing the ratio of ligands **1**, **3**, and $[Cu(MeCN)_4]PF_6$ to 1:1:1 caused a visible color difference and block shaped red crystals of $\mathbf{C1}^{(II)}$ were isolated by slow diffusion of diethyl ether into a dichloromethane solution of the complex. X-ray analysis revealed the formation of a *zigzag* chain structure. Each of the Cu^+ ions is now tetrahedrally coordinated by four N atoms with ligation from phenanthroline **1** and two pyridines, the latter stemming from two different molecules of **3**. As depicted in Figure 3, the *zigzag* chains are arranged in a side-by-side manner to produce a 2D array along the *ac* plane, showing extensive $\pi-\pi$-stacking interactions (3.69 Å) between the phenanthroline moiety and a pyridine ring of the neighboring array. Close inspection of the copper(I) centers in an individual chain in $\mathbf{C1}^{(II)}$ divulges that, unlike in $\mathbf{C1}^{(I)}$, the pyridine rings are not positioned in the shielding region of **1**. The steric hindrance between the mesityl groups and the pyridine ortho protons enforces the loss of ligand coplanarity in **3** promoting the more common tetrahedral (albeit distorted) geometry at the copper(I) center.

The above structural alteration from a discrete heteroleptic assembly in $\mathbf{C1}^{(I)}$ to a polymeric chain structure in $\mathbf{C1}^{(II)}$ by changing the stoichiometric ratio of $[Cu(\mathbf{1})]^+$/ **3** may therefore be viewed as a supramolecular modification, whereby the geometry (and coordination number) of the involved copper(I) center expands from trigonal (3) to tetrahedral (4) in the solid state.

To explore the effects of the counteranion on the HETPYP-I complex formation, the above reaction was modified by using

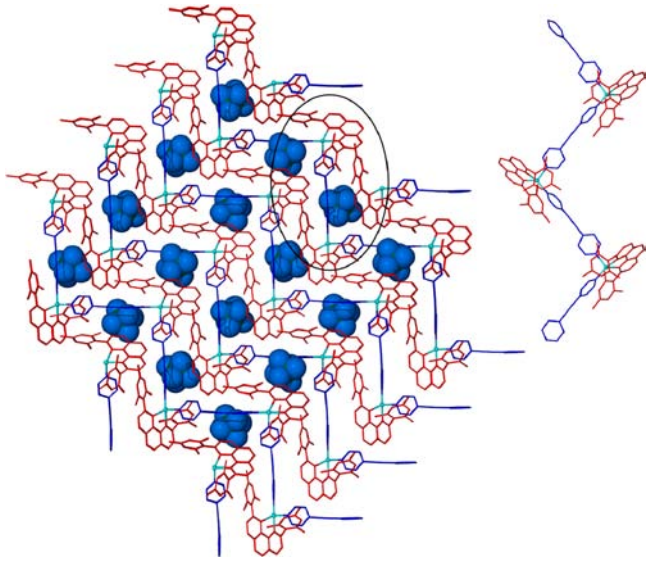

Figure 3. View of the 2D packing arrangement of complex $\mathbf{C1}^{(II)}$ with PF_6^- anions (shown in a space filling mode) inside the channel. Inset shows the *zigzag* motif of an individual chain structure. Hydrogen atoms were omitted for clarity. Color code: **1**, red; **3**, blue; copper, cyan.

the $[Cu(CF_3SO_3)(toluene)]$ complex as a copper(I) source. Complexation was carried out in dichloromethane by reacting $[Cu(\mathbf{1})]^+$/**3** in a 2:1 ratio affording complex **C2**, from which single crystals were grown as red needles by slow evaporation of dichloromethane. The X-ray analysis reveals that the metal ion is bound to two nitrogens of phenanthroline **1** (2.10 Å and 2.00 Å) and one nitrogen atom of ligand **3** (1.93 Å), while the fourth coordination site is now filled at 2.34 Å distance with one oxygen atom of the triflate anion, leading to a distorted tetrahedral geometry at each copper(I) center (Figure 4). The overall structure of complex **C2** was found to be quite similar to that of complex $\mathbf{C1}^{(I)}$ considering the spatial orientation of ligands **1** and **3**, except that the central copper(I) ion is now tetra-coordinated. Strong $\pi-\pi$ stacking interactions exist between the pyridine ring and one of the mesityl groups of ligand **1** (3.63 Å). On the basis of the above results, we conclude that the complexation scenario, i.e. trigonal vs tetrahedral coordination at the copper(I) center, depends on the properties of the anion furnishing weak or strong binding.

Self-Assembly of ***2*** *and [Cu(1)]$^+$ (Complexes* $C3^{(I)}$ *and* $C3^{(II)}$*).* To evaluate the impact of shortening the distance between two nitrogen donor centers in the bipyridine and thus an increasing steric repulsion between the caps, **3** is replaced by the shorter bipyridine **2** (Scheme 2). We envisaged that the smallest heteroleptic assembly formed at lowest entropic costs following the HETPYP-I strategy ($[Cu(\mathbf{1})]^+$/**2** = 2:1) should be $[Cu_2(\mathbf{1})_2(\mathbf{2})]^{2+}$. Unfortunately, though single crystals of relatively big size and good shape were obtained by different methods, all crystals proved to be unstable during diffraction measurements. Nevertheless, formation of the desired complex $\mathbf{C3}^{(I)}$ was attested by the ESI-FTICR mass spectrometry data, with the molecular ion being readily detected by its correct isotopic pattern and exact mass (see Supporting Information, Figure S12).

In another set of experiments, addition of 1 equiv of **2** to a 1:1 mixture of **1** and $[Cu(MeCN)_4]PF_6$ in dichloromethane caused a conversion from $\mathbf{C3}^{(I)} \rightarrow \mathbf{C3}^{(II)}$, as revealed by the resulting solid state structure. Small red crystals of complex

dx.doi.org/10.1021/ic301286w | *Inorg. Chem.* 2012, 51, 10832−10841

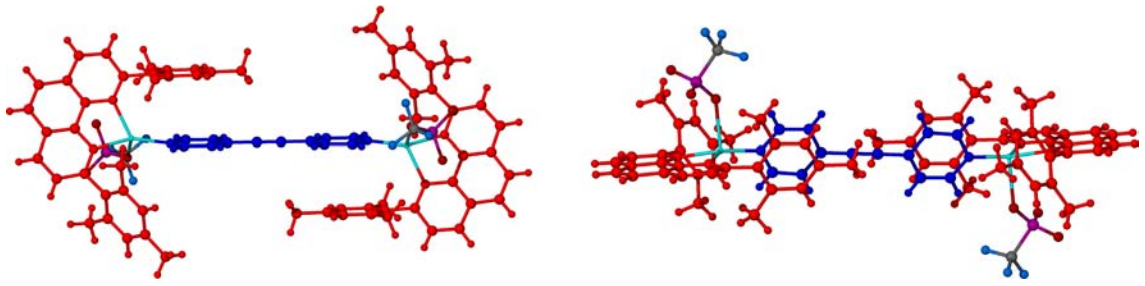

Figure 4. Side view (left) and top view (right) of the crystal structure for complex **C2**.

$\mathbf{C3}^{(II)}$, suitable for X-ray analysis, were obtained by a method similar to that used for $\mathbf{C1}^{(II)}$. The solid state structure of $\mathbf{C3}^{(II)}$ reveals that each copper(I) center is tetrahedrally bound to both nitrogens of one phenanthroline and two nitrogen atoms belonging to different bipyridine ligands. The overall structure can be viewed as a one-dimensional (1D) chain arrangement with the $[Cu(\mathbf{1})]^+$ motif acting as a capping unit and the 4,4′-bipyridine ligand extending the framework (Figure 5). The

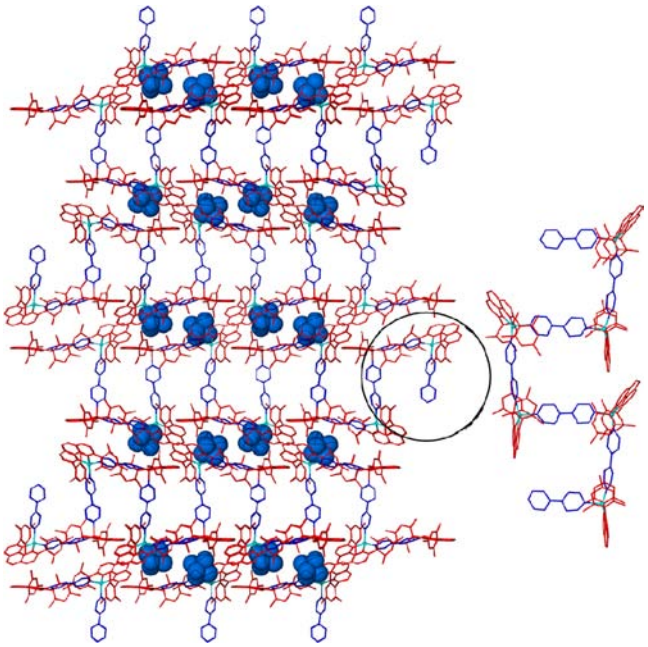

Figure 5. Crystal packing of complex $\mathbf{C3}^{(II)}$ along *c* axis, with PF_6^- anions (shown in space filling mode) located in between the 2D layers. Inset shows the twist in the chain structure. Color code: **1**, red; **2**, blue; copper, cyan. All hydrogen atoms were omitted for clarity.

structure of $\mathbf{C3}^{(II)}$ is different from the zigzag chain structure of $\mathbf{C1}^{(II)}$ in a way that the neighboring bipyridines **2** to the $[Cu_2(\mathbf{1})_2\mathbf{2}]$ building block unit are aligned in a syn−anti−syn−anti orientation (Cu1−Cu2−Cu3−Cu4 = 7.7° and Cu2−Cu3−Cu4−Cu5 = 179.4°), providing a notable twist to the polymer chain (Figure 5, inset), whereas in the later structure $\mathbf{C1}^{(II)}$, the longer bipyridines **3** run always anti (Cu1−Cu2−Cu3−Cu4 = 180.0°). Both structures are different from the helicate structure reported previously.[15]

Self-Assembly of **4** *and* $[Cu(1)]^+$ *(Complex* $C4^{(I)}$ = $[Cu_3(1)_3(\mathbf{4})](PF_6)_3$*).* To probe the formation of a trifold HETPYP-I complex with three $[Cu(\mathbf{1})]^+$ caps on a tripyridine ligand to afford a $[Cu_3(phenAr_2)_3(py)]^{3+}$ assembly (here, py represents a tripyridine ligand), the reaction of the $[Cu(\mathbf{1})]^+$ complex with ligand **4** (Scheme 2) was initiated. Single crystals were grown as orange blocks by diffusion of diethyl ether into a dichloromethane solution of capped $[Cu(\mathbf{1})]^+$ complex and ligand **4** (at 3:1 ratio). The crystals are very sensitive to air and loose crystallinity immediately when taken out of the mother liquor. Data collection could only be done at low temperature by wrapping in oil prior to mounting. The coordination environment about the copper(I) ions in $\mathbf{C4}^{(I)}$ follows a distorted trigonal geometry with ligation from two N atoms of **1** and one pyridine N atom of **4**. In $\mathbf{C4}^{(I)}$, the tripyridine ligand adopts a nearly planar molecular structure joining three crystallographically independent $[Cu(\mathbf{1})]^+$ centers using its long aromatic arms. The PF_6^- anion (5.1 Å) and dichloromethane solvent molecule (4.9 Å) are quite far away from any metal ion and are hence not bound to Cu^+ (Supporting Information, Figure S32). A wide variation of bond distances and bond angles is observed at the three Cu^+−N(py) units, although they lie within a range observed in other Cu^+−N(pyridine) structures.[15,27] Figure 6 represents a view of the

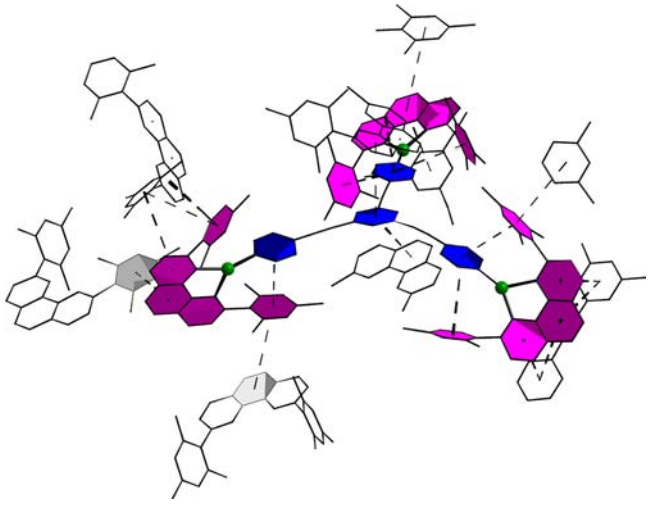

Figure 6. A perspective view of $\mathbf{C4}^{(I)}$ showing intra- and intermolecular secondary interactions. Solvent molecules, anions, and hydrogen atoms are omitted for clarity.

discrete assembly of $\mathbf{C4}^{(I)}$ down the *c* axis, accentuating the Y-like arrangement of all Cu^+ ions and the 180° rotation of every alternate phenanthroline ring along the *b* axis. In this structure, the phenanthroline ligands are oriented with respect to each other in such a way that the "bottom side" of ligand **1** may come into contact (3.5 Å) with another aromatic plane of the neighboring assembly to maximize $\pi-\pi$ stacking. This turns the phenanthroline rings slightly offset and causes an unusual trigonal distortion at the copper(I) center.

dx.doi.org/10.1021/ic301286w | *Inorg. Chem.* 2012, 51, 10832−10841

Mimicking the Solid State Structure of $C4^{(II)}$ = $[Cu_3(1)_3(4)_2]^{3+}$. The reaction of $[Cu(1)]^+$ and ligand **4** (3: 2 molar ratio) furnished a molecular assembly in solution that is denoted as $C4^{(II)}$ in the following. Since all efforts to grow single crystals of $C4^{(II)}$ remained unsuccessful, we substituted ligand **4** by its methylated congener 4_{Me} (see Scheme 2). Reaction of 4_{Me} and $[Cu(1)]^+$ in a 2: 3 molar ratio in dichloromethane-d_2 furnishes an ^{1}H NMR spectrum that is identical to the spectrum of the assembly $C4^{(II)}$, except for the additional methyl groups (see Figure S21 in the Supporting Information). The full agreement of the solution state NMR characteristics of $C4^{(II)}$ and $C4_{Me}{}^{(II)}$ suggests that the solid state assembly $C4^{(II)}$ should be well represented by that of $C4_{Me}{}^{(II)}$ = $[Cu_3(1)_3(4_{Me})_2]^{3+}$ that is literature known.[15] The latter structure (Figure 7, another view of the honeycomb structure

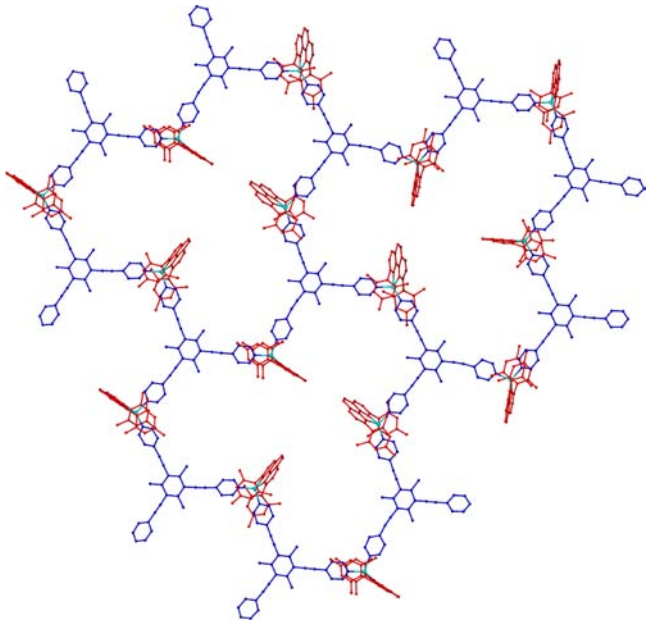

Figure 7. Top view of honeycomb like two-dimensional arrangement in $C4_{Me}{}^{(II)}$.[15] Color code: **1**, red; 4_{Me}, blue; copper, cyan. All H-atoms, anions and solvate molecules were omitted for clarity.

in the original paper) is characterized by a broken honeycomb network, where every individual $[Cu(1)]^+$ cap is connected with two pyridines stemming from two different ligands 4_{Me}, resulting in a tetrahedral arrangement at each copper(I) center.

The above annotations have successfully demonstrated that for various combinations of $[Cu(1)]^+$ and oligopyridines, that is, **1**−**4**, the stoichiometric ratio reliably commands the outcome of the solid state structure resulting in either a discrete HETPYP-I or oligomeric HETPYP-II structure. The present study further indicates the important role that weakly coordinating counterions may play in such supramolecular structure alteration.

Solution State Studies. *Self-Assembly of Bipyridine* **3** *and* $[Cu(1)]^+$ *in Solution.* At first, an oligomeric coordination scenario, as detected in all solid-state HETPYP-II assemblies, seems rather unlikely in solution due to the unfavorable entropic costs. We thus studied how HETPYP-I and HETPYP-II assemblies would manifest themselves in solution.

As a representative example for all cases studied so far, the structure of $C1^{(I)}$ and $C1^{(II)}$ in CD_2Cl_2 was intimately analyzed. The ^{1}H NMR spectrum of $C1^{(I)}$ reveals only one set of sharp signals, with the chemical shifts of the pyridine α and β protons of **3** (for the numbering of the protons, see Scheme 2) being drastically moved from 8.63 to 7.00 ppm and from 7.43 to 7.20 ppm, respectively (Table 2). Such finding is in line with the

Table 2. Diagnostic Shifts for Pyridine Protons in Various HETPYP-I and HETPYP-II Structures

complex[a]	δ^b (H_α)	$\Delta\delta$ (H_α)^{b,c}	δ^b (H_β)	$\Delta\delta$ (H_β)^{b,c}
$C1^{(I)}$	7.00	0.68	7.20	0.09
$C1_S{}^{(II)}$	7.68		7.29	
$C3^{(I)}$	7.17	0.61	7.32	0.07
$C3_S{}^{(II)}$	7.78		7.39	
$C4^{(I)}$	6.88	0.76	7.18	0.11
$C4_S{}^{(II)}$	7.64		7.29	

[a]Recorded in CD_2Cl_2. [b]In ppm. [c]^{1}H NMR shift difference for H_α or H_β between $Cn_S{}^{(II)}$ and $Cn^{(I)}$.

symmetric encapsulation of the pyridine rings into the cavity of the electron-rich mesityl groups of **1**. 3-H and 4-H protons (see Scheme 2) of the phenanthroline residue are downfield shifted to 7.94 and 8.72 ppm, respectively, due to metal complexation. DOSY NMR indicates the formation of a single species in solution (Supporting Information). ESI-FTICR mass spectra obtained at very soft ionization conditions provide a clear clue for the existence of a discrete assembly in the gas phase as they show signals corresponding to the molecular ion of $C1^{(I)}$ in its singly charged form $[Cu_2(1)_2(3)(PF_6)]^+$ at m/z = 1285.3 with correct isotopic pattern and exact mass (Supporting Information, Figure S3). Nevertheless, a significant amount of fragmentation by loss of the neutral complex $[Cu(1)(PF_6)]$ turned out to be inevitable, leading to the base peak at m/z 659.2, which is assigned to the heteroleptic mononuclear species $[Cu(1)(3)]^+$. According to the gas-phase results, the strongly bound $[Cu(1)]^+$ entities of $C1^{(I)}$ stay intact, while the significantly weaker bound pyridine ligands dissociate off in the presence of excess energy.

Changing the ratio of ligands **1**, **3**, and $[Cu(MeCN)_4]PF_6$ to 1:1:1 leads to a shift of the pyridine α and β protons of **3** from 8.63 to 7.68 ppm and from 7.43 to 7.29 ppm, respectively, a much smaller upfield shift in comparison to that found for $C1^{(I)}$. The ^{1}H NMR spectrum therefore points toward the formation of an aggregate containing other structural elements. Clearly, both α and β pyridine protons experience less shielding from the mesityl group of **1**. Although the ESI-FTICR MS (even under very soft ionization condition) exhibits only signals of small fragments due to weak $[Cu_2(3)]^{2+}$---N(py) bonding, the DOSY spectrum shows a single species (Supporting Information). Surprisingly, the diffusion coefficient of the aggregate derived from DOSY ($D = 10.2 \times 10^{-10}$ m^2 s^{-1}; r_H = 0.51 nm) was found to be larger than that for $C1^{(I)}$ ($D = 8.6 \times 10^{-10}$ m^2 s^{-1}; r_H = 0.60 nm). These numbers suggest that the HETPYP assembly at a ratio of $[Cu(1)]^+$/ **3** = 1: 1 ought to be smaller in solution than $C1^{(I)}$. To resolve this issue, dynamic light scattering (DLS) measurements were undertaken in dichloromethane. The DLS data reveal a monomodal size distribution for both assemblies (Supporting Information, Figure S8) allowing to establish the hydrodynamic diameter as d = 1.12 nm (for the unknown assembly at a ratio of $[Cu(1)]^+$/ **3** = 1: 1) and 1.30 nm (for $C1^{(I)}$). Both diameters are in full agreement with the size determination from the DOSY NMR (Supporting Information, Table S2). Assessing several different possible arrangements of ligand **3** and the

dx.doi.org/10.1021/ic301286w | Inorg. Chem. 2012, 51, 10832−10841

$[Cu(\mathbf{1})]^+$ cap at a ratio 1:1, the simplest model according to Occam's razor is the one in which a $[Cu(\mathbf{1})]^+$ cap is only attached to one pyridine of ligand **3** with the other pyridine of the same ligand remaining uncoordinated (Scheme 3, a and b).

Scheme 3. Possible Associations of Bipyridine 3 with the Capped $[Cu(\mathbf{1})]^+$ Complex, When Used in 1:2 and 1:1 Stoichiometry in Solution[a]

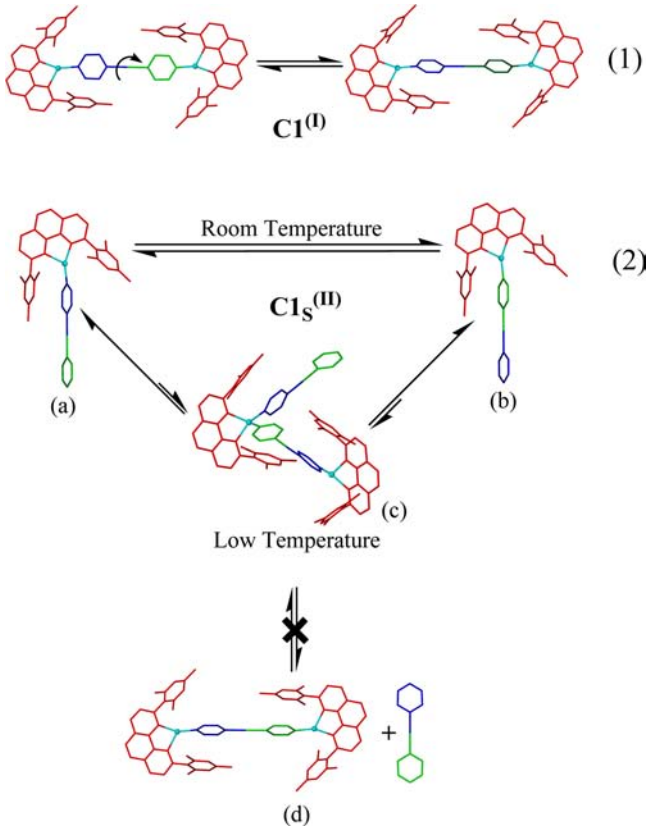

[a]To show the exchange processes, the two pyridine rings of **3** are colored differently.

Most likely, the copper(I) center in $[Cu(\mathbf{1})(\mathbf{3})]^+$ is coordinated in a trigonal fashion as in $\mathbf{C1}^{(I)}$. Because of very rapid exchange, the average pyridine NMR resonance are placed almost halfway (Table 2 and Figure S8 in Supporting Information) between that of $\mathbf{C1}^{(I)}$ and **3**. This model is furthermore justified because the room temperature ^{1}H NMR spectrum of the aggregate exhibits no signals of a free ligand **3**. Thus, an equilibrium involving species d, as depicted in Scheme 3, seems unlikely.

Further insight was obtained upon probing the mixture $[Cu(\mathbf{1})]^+$/ **3** at ratios 1:1 and 2:1 ($=\mathbf{C1}^{(I)}$) using different temperatures (Figure 8). Upon decreasing the temperature of the $\mathbf{C1}^{(I)}$ assembly, only the pyridine α protons experience a pronounced upfield shift (from 7.00 ppm at 25 °C to 6.20 ppm at −80 °C) associated with incessant peak sharpening. None of the phenanthroline protons changes its shift, which indicates that the phen-Cu^+-py linkage remains intact. Thus, the observations suggest that the $\mathbf{C1}^{(I)}$ assembly is dynamic at room temperature due to rotation about the long axis of **3** (see process (1) in Scheme 3). Once the temperature reaches −80 °C, a more rigid conformation is attained, in which the pyridine α protons experience strong shielding effects by the mesityl groups.

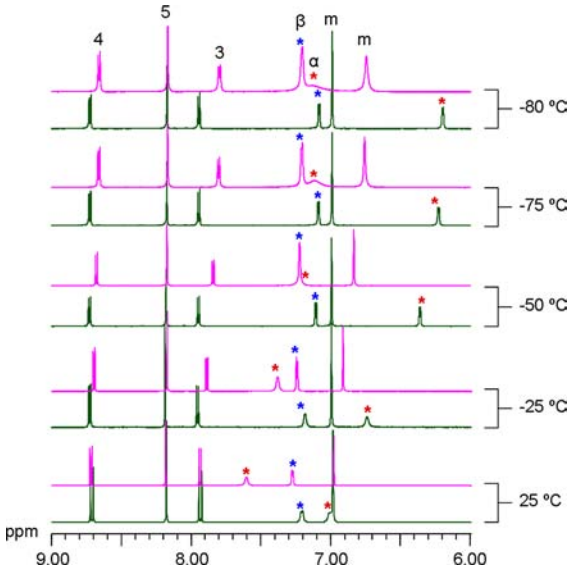

Figure 8. Variable temperature ^{1}H NMR spectra (partial spectrum) of $\mathbf{C1}^{(I)}$ and $\mathbf{C1_S}^{(II)}$, all in CD_2Cl_2. Color code: $\mathbf{C1}^{(I)}$, green; $\mathbf{C1_S}^{(II)}$, pink; py_α, red stars; py_β, blue stars.

Quite in contrast, the assembly at $[Cu(\mathbf{1})]^+$/ **3** = 1:1 shows notable upfield shifts of both the phenanthroline and pyridine α protons upon lowering the temperature. The pyridine α protons experience progressive upfield shifts and finally end up as broad singlet at −80 °C. At this temperature, the pyridine protons reveal a shift close to that of the HETPYP-I scenario (Figure 8). However, no peaks corresponding to free ligand **3** are observed, which excludes scenario d in eq 2 (Scheme 3). Because both pyridine terminals of **3** experience the same NMR signal shift at all temperatures, the bipyridine terminals have rapidly to exchange their environment by detaching and reattaching to the copper caps (assembly a and b in Scheme 3). At −80 °C, this swapping motion is becoming slower as seen from the pyridine α protons that show peak broadening by coalescence. With decreasing temperature, the mesityl hydrogens experience a significant upfield shift that should be indicative for a tetracoordination at copper.[17,18] Considering a free energy balance between enthaplic gain through maximum site occupancy and entropic costs, we thus expect the solution assembly of $[Cu(\mathbf{1})]^+$/ **3** = 1:1 at −80 °C to shift more and more toward structure (c) either as a dimeric or even oligomeric entity (Scheme 3). Notably, the latter structure closely resembles a subpart of the solid state structure of $\mathbf{C1}^{(II)}$.

Clearly, the solution structure of $[Cu(\mathbf{1})]^+$/ **3** = 1:1 is complex and temperature dependent. Thus, in the following this aggregate in solution will be denoted as $\mathbf{C1_S}^{(II)}$. It seems that at room temperature the structure is best described as a complex $[Cu(\mathbf{1})(\mathbf{3})]^+$ with one pyridine terminal of **3** left uncoordinated (see a + b in Scheme 3), while at low temperature due to decreasing entropic costs of larger aggregates, we see a shift toward a dimeric or even oligomeric structure that is largely similar to the polymeric solid state structure.

The dynamic nature of the $\mathbf{C1_S}^{(II)}$ assembly is further corroborated by a ^{1}H NMR titration experiment, showing that after addition of one equivalent $[Cu(\mathbf{1})]^+$ to a solution of $\mathbf{C1_S}^{(II)}$, the original spectrum of $\mathbf{C1}^{(I)}$ is fully reconstituted (Supporting Information, Figure S7).

dx.doi.org/10.1021/ic301286w | Inorg. Chem. 2012, 51, 10832−10841

For the other systems as well, that is, $\mathbf{Cn_S}^{(II)}$ and $\mathbf{Cn}^{(I)}$, a fully analogous behavior may be derived from their ^{1}H NMR data (Table 2) and in some cases is further supported by DOSY and DLS measurements (see Supporting Information, Table S2). The analogy of all systems is best read out from the $\Delta\delta$ (H_α) values that represent the difference of δ (H_α) of HETPYP-I and HETPYP-II assemblies. For all pairs $\mathbf{Cn_S}^{(II)}$ and $\mathbf{Cn}^{(I)}$ with n = 1, 3, and 4, the $\Delta\delta$ value is remarkably constant.

Thus, the solution structure of all $\mathbf{Cn_s}^{(I)}$ is best represented by that of the discrete species $\mathbf{Cn}^{(I)}$ as documented through solid state analysis. Using the insight received on system $\mathbf{C1_S}^{(II)}$, however, it is clear that for other $\mathbf{Cn_s}^{(II)}$, as well a tetracoordinated copper(I) center, that is, a HETPYP-II structure, is only plausible at rather low temperature. At room temperature, tetracoordination is no longer thermochemically competitive, because any oligomeric assembly would generate too high entropic costs ($-T\Delta S$). Obviously, the entropic costs of copper(I) tetracoordination in the solid state are much less relevant as the observed polymeric structure is strongly supported by extensive interlayer $\pi-\pi$ stacking interactions because of the parallel packing of the one-dimensional chains.

CONCLUSION

In conclusion, the aforementioned results in solution, solid state and gas phase demonstrate the successful utilization of 2,9-dimesityl phenanthroline as a cap for tricoordinated copper(I) centers in heteroleptic $[Cu_n(phenAr_2)_n(py)]^{n+}$ assemblies, by choosing the appropriate di- and tripyridyl ligands, using the HETPYP protocol. Based on solid state evidence, we see a stoichiometry-dependent structural changeover, with the concomitant coordination at copper(I) changing from trigonal (HETPYP-I) to tetrahedral (HETPYP-II) depending on the amount of pyridine ligands. While HETPYP-I derived species $\mathbf{Cn}^{(I)}$ are discrete supramolecules both in solid state and solution, the HETPYP-II assemblies $\mathbf{Cn}^{(II)}$ are characterized by their polymeric nature in the solid. In solution, there is a structural changeover depending on the temperature. At low temperature, the "di- and oligomeric" solution structure is reminiscent of the solid-state structure, but it breaks down to "monomeric" $[Cu(\mathbf{1})(\mathbf{3})]^+$ units at higher temperature due to entropic reasons.

The dynamic nature of both assemblies in solution was proven by the reversible interconversion of $\mathbf{Cn_S}^{(I)}$ and $\mathbf{Cn_S}^{(II)}$ assemblies upon titration with the required components. Such dynamic modulation may allow to introduce novel stimuli-dependent properties, a particularly attractive feature of functional dynamic materials, for example through modifying constitution by exchange and reshuffling components.

EXPERIMENTAL SECTION

General Methods. All commercial reagents were used without further purification. The purification and drying of the solvents was accomplished according to standard protocols. Confirmation of the structures of all products was obtained by ^{1}H NMR and ^{13}C NMR spectroscopy (Bruker Avance 400 spectrometer) as well as DOSY NMR (Varian VNMR-S 600 MHz spectrometer) using the deuterated solvent as the lock and residual solvent as the internal reference. The following abbreviations were utilized to describe peak patterns: s = singlet, d = doublet, t = triplet, dd = doublet of doublet, br = broad and m = multiplet. Numbering of carbon atoms of the molecular formulas shown in the Experimental Section is used only for assignments of the NMR signal and is not in accordance with the IUPAC nomenclature rules. Melting points were measured on a Büchi SMP-20 instrument and are uncorrected. Infrared spectra were recorded on a Perkin-Elmer 1750 FT-IR spectrometer with the software of IRDM 1700. Elemental analysis measurements were done using the EA 3000 CHNS. Mass spectra were recorded on a Bruker APEX IV Fourier transform ion cyclotron resonance (FT-ICR) mass spectrometer. Dynamic light scattering (DLS) data were acquired at 20 °C in dichloromethane on a Malvern Zetasizer (Zetasizer Nano, Malvern Instruments GmbH, Germany).

X-ray Structural Studies. For complexes $\mathbf{C1}^{(I)}$, $\mathbf{C1}^{(II)}$, **C2**, and $\mathbf{C4}^{(I)}$: Data collection, Bruker APEX2; cell refinement, Bruker SAINT;[29] data reduction, Bruker SAINT. Program used to solve structure: SHELXS97.[30] Program used to refine structure: SHELXL97.[30] Molecular graphics: Bruker SHELXTL.[31] Software used to prepare material for publication: Bruker SHELXTL. The X-ray single-crystal diffraction data for complex $\mathbf{C3}^{(II)}$ was collected on a SIEMENS SMART diffractometer. The structures were solved using SHELXS-97[30] and refined by full-matrix least-squares analysis. Hydrogen atoms were generated theoretically onto the specific atoms and refined isotropically with fixed thermal factors. The non-H atoms were refined with anisotropic thermal parameters (for details see Supporting Information). CCDC reference nos. 836993−836996 contain the supplementary crystallographic data of $\mathbf{C1}^{(I)}$, $\mathbf{C1}^{(II)}$, **C2**, and $\mathbf{C4}^{(I)}$. The data can also be obtained free of charge at www.ccdc.cam.ac.uk/conts/retrieving.html [or from the Cambridge Crystallographic Data Centre, 12, Union Road, Cambridge CB2 1EZ, UK; Fax: (Internet.)+44−1223/336−033; E- mail:deposit@ccdc.cam.ac.uk].

Synthesis and Characterization of $\mathbf{C1}^{(I)}$. Ligand **1**[15] (4.16 mg, 10.0 μmol) and $[Cu(MeCN_4)]PF_6$ (3.73 mg, 10.0 μmol) were dissolved in dichloromethane (0.50 mL) affording a slightly yellow solution. Then, **3**[10] (0.90 mg, 5.0 μmol) was added resulting in an orange solution. After removal of the solvents, the solid residue was analyzed without any further purification. Single crystals, suitable for X-ray study, were grown by slow diffusion of diethylether into a 1,2-dichlorobenzene solution of $\mathbf{C1}^{(I)}$. For the solid state characterization, see X-ray structural analysis. Yield: quantitative. mp = 148 °C. IR (KBr): ν = 2918, 2857, 1612, 1586, 1508, 1481, 1426, 1381, 1361, 1298, 1216, 1148, 1111, 1030, 841, 651, 625, 557 cm^{-1}. ^{1}H NMR (400 MHz, CD_2Cl_2): δ = 8.72 (d, J = 8.3 Hz, 4H, 4-H), 8.18 (s, 4H, 5-H), 7.94 (d, J = 8.3 Hz, 4H, 3-H), 7.20 (d, J = 5.1 Hz, 4H, β-H), 7.00 (d, J = 5.1 Hz, 4H, α-H), 6.98 (s, 8H, m-H), 2.36 (s, 12H, b-H) 2.04 (s, 24H, a-H). ^{13}C NMR (100 MHz, CD_2Cl_2): δ = 161.0, 150.2, 144.0, 140.0, 139.9, 137.3, 136.2, 132.0, 129.2, 128.3, 127.6, 127.3, 127.2, 92.2, 21.2, 20.5. FTICR-MS Calcd. for $[Cu_2(\mathbf{1})_2(\mathbf{3})(PF_6)]^+$: m/z 1285.3; found m/z 1285.3. Anal.Calcd for $C_{72}H_{64}Cu_2F_{12}N_6P_2{\cdot}0.5CH_2Cl_2$ = ($[Cu_2(\mathbf{1})_2(\mathbf{3})(PF_6)_2]{\cdot}0.5CH_2Cl_2$): C, 59.12; H, 4.45; N, 5.71. Found: C, 59.19; H, 4.67; N, 5.39.

Synthesis and Characterization of $\mathbf{C3}^{(I)}$. Ligand **1** (4.16 mg, 10.0 μmol) and $[Cu(MeCN_4)]PF_6$ (3.73 mg, 10.0 μmol) were dissolved in dichloromethane (0.50 mL) affording a slightly yellow hue. Then, **2** (0.78 mg, 5.0 μmol) was added resulting in an orange solution. After removal of the solvents the solid residue was analyzed without any further purification. Yield: Quantitative. mp: 135 °C. IR (KBr): ν = 2919, 2858, 1609, 1505, 1482, 1444, 1410, 1379, 1356, 1297, 1217, 1147, 1110, 1067, 840, 625, 558 cm^{-1}. ^{1}H NMR (400 MHz, CD_2Cl_2): δ = 8.72 (d, J = 8.3 Hz, 4H, 4-H), 8.18 (s, 4H, 5-H), 7.95 (d, J = 8.3 Hz, 4H, 3-H), 7.32 (br, 4H, β-H), 7.17 (br, 4H, α-H), 6.98 (s, 8H, m-H), 2.33 (s, 12H, b-H) 2.04 (s, 24H, a-H). ^{13}C NMR (100 MHz, CD_2Cl_2): δ = 160.9, 151.0, 145.6, 144.0, 139.7, 139.5, 137.4, 136.2, 129.1, 128.4, 127.5, 127.2, 122.1, 116.9 (CN of acetonitrile), 21.2, 20.4, 2.0 (CH_3 of acetonitrile). FTICR-MS Calcd. for $[Cu_2(\mathbf{1})_2(\mathbf{2})(PF_6)]^+$: m/z 1259.3; found m/z 1259.3. Anal. Calcd. for $C_{70}H_{64}Cu_2F_{12}N_6P_2$ $[Cu_2(\mathbf{1})_2(\mathbf{2})(PF6)_2]$: C, 59.78; H, 4.59; N, 5.98. Found: C, 59.44; H, 4.98; N, 6.13.

Synthesis and Characterization of $\mathbf{C4}^{(I)}$. Ligand **1** (4.16 mg, 10.0 μmol) and $[Cu(MeCN_4)]PF_6$ (3.73 mg, 10.0 μmol) were dissolved in dichloromethane (0.50 mL) assuming a slightly yellow color. Then, **4**[14d] (1.27 mg, 3.33 μmol) was added resulting in an orange solution. After removal of the solvents, the solid residue was analyzed without any further purification. Single crystals suitable for X-ray analysis were obtained by slow diffusion of diethylether into a

dichloromethane solution of **C4**$^{(I)}$. For the solid state characterization, see the X-ray structural analysis. Yield: quantitative. mp: 220 °C. IR (KBr): ν = 2917, 2857, 2215, 1608, 1587, 1558, 1480, 1425, 1380, 1359, 1296, 1215, 1147, 1110, 1030, 840, 650, 624, 557 cm^{-1}. ^{1}H NMR (400 MHz, CD_2Cl_2): δ = 8.72 (d, J = 8.3 Hz, 6H, 4-H), 8.18 (s, 6H, 5-H), 7.94 (d, J = 8.3 Hz, 6H, 3-H), 7.88 (s, 3H, c-H), 7.18 (br, 6H, β-H), 6.99 (s, 12H, m-H), 6.88 (br, 6H, α-H), 2.38 (s, 18H, b-H) 2.04 (s, 36H, a-H). ^{13}C NMR (100 MHz, CD_2Cl_2): δ = 161.0, 150.1, 144.0, 139.9, 139.7, 137.3, 136.3, 136.2, 132.9, 129.2, 128.3, 127.6, 127.2, 126.9, 123.4, 116.9 (CN of acetonitrile), 94.4, 87.6, 21.2, 20.5, 2.08 (CH_3 of acetonitrile). FTICR-MS: Calcd. for $[Cu_3(\mathbf{1})_3(\mathbf{4})(PF_6)]^{2+}$: m/z 983.3; found m/z 983.3. Anal. Calcd. for $C_{117}H_{99}Cu_3F_{18}N_9P_3$·MeCN ($[Cu_3(\mathbf{1})_3(\mathbf{4})(PF_6)_3]$·MeCN): C, 62.21; H, 4.47; N, 6.10. Found: C, 62.42; H, 4.60; N, 6.24.

■ ASSOCIATED CONTENT

Supporting Information

Experimental details of synthesis, characterization for all **Cn**$^{(II)}$, **Cn$_S$**$^{(II)}$, and **C2** complexes, NMR spectra, DLS, FT-IR and mass spectrometric data, views of the single crystal X-ray structures. X-ray crystallographic data for **C1**$^{(I)}$, **C1**$^{(II)}$, **C2**, **C3**$^{(II)}$, and **C4**$^{(I)}$ in CIF format are provided. This material is available free of charge via the Internet at http://pubs.acs.org.

■ AUTHOR INFORMATION

Corresponding Author

*E-mail: schmittel@chemie.uni-siegen.de.

Notes

The authors declare no competing financial interest.

■ ACKNOWLEDGMENTS

We are indebted to the DFG for continued support and to the Alexander von Humboldt Foundation for a stipend to S.N. We thank Dr. J. W. Bats (Frankfurt) for measuring the X-ray data of **C3**$^{(II)}$.

■ REFERENCES

(1) (a) Lehn, J.-M. *Supramolecular Chemistry: Concepts and Perspectives*; VCH: Weinheim, Germany, 1995. (b) Batten, S. R.; Robson, R. *Angew. Chem., Int. Ed.* **1998**, 37. (c) Atwood, J. L.; Steed., J. W. *Encyclopedia of Supramolecular Chemistry*; Marcel Dekker Ltd.: New York, 2004.

(2) (a) Ghosh, K.; Yang, H.-B; Northrop, B. H.; Lyndon, M. M.; Zheng, Y.-R.; Muddiman, D. C.; Stang, P. J. *J. Am. Chem. Soc.* **2008**, *130*, 5320. (b) Zhao, L.; Ghosh, K.; Zheng, Y.; Lyndon, M. M.; Williams, T. I.; Stang, P. J. *Inorg. Chem.* **2009**, *48*, 5590. (c) Lee, J.; Ghosh, K.; Stang., P. J. *J. Am. Chem. Soc.* **2009**, *131*, 12028. (d) Kikuchi, T.; Sato, S.; Fujita, M. *J. Am. Chem. Soc.* **2010**, *132*, 15930. (e) Inokuma, Y.; Kawano, M.; Fujita, M. *Nat. Chem.* **2011**, *3*, 349.

(3) (a) Mahata, K.; Schmittel, M. *J. Am. Chem. Soc.* **2009**, *131*, 16544. (b) Jiang, W.; Schalley, C. A. *Proc. Natl. Acad. Sci. U.S.A.* **2009**, *106*, 10425. (c) Schmittel, M.; Samanta, S. K. *J. Org. Chem.* **2010**, *75*, 5911. (d) Mahata, K.; Saha, M. L.; Schmittel, M. *J. Am. Chem. Soc.* **2010**, *132*, 15933. (e) Jiang, W.; Schäfer, A.; Mohr, P. C.; Schalley, C. A. *J. Am. Chem. Soc.* **2010**, *132*, 2309. (f) Jiang, W.; Nowosinski, K.; Löw, N. L.; Dzyuba, E. V.; Klautzsch, F.; Schäfer, A.; Huuskonen, J.; Rissanen, K.; Schalley, C. A. *J. Am. Chem. Soc.* **2012**, *134*, 1860.

(4) (a) Cairns, A. J.; Perman, J. A.; Wojtas, L.; Kravtsov, V. C.; Alkordi, M. H.; Eddaoudi, M.; Zaworotko, M. J. *J. Am. Chem. Soc.* **2008**, *130*, 1560. (b) Sun, Q.-F.; Iwasa, J.; Ogawa, D.; Ishido, Y.; Sato, S.; Ozeki, T.; Sei, Y.; Yamaguchi, K.; Fujita, M. *Science* **2010**, *328*, 1144. (c) Li, D.; Zhou, W.; Landskron, K.; Sato, S.; Kiely, C. J.; Fujita, M.; Liu, T. *Angew. Chem., Int. Ed.* **2011**, *50*, 5182.

(5) (a) Abad-Zapatero, C.; Abdel-Meguid, S. S.; Johnson, J. E.; Leslie, A. G. W.; Rayment, I.; Rossmann, M. G.; Suck, D.; Tsukihara, T. *Nature* **1980**, *286*, 33. (b) Rossmann, M. G.; Arnold, E.; Erickson, J. W.; Frankenberger, E. A.; Griffith, J. P.; Hecht, H.-J.; Johnson, J. E.; Kamer, G.; Luo, M.; Mosser, A. G.; Rueckert, R. R.; Sherry, B.; Vriend, G. *Nature* **1985**, *317*, 145.

(6) (a) Angurell, I.; Ferrer, M.; Gutiérrez, A.; Martínez, M.; Rodríguez, L.; Rossell, O.; Engeser, M. *Chem.—Eur. J.* **2010**, *16*, 13960. (b) Saha, M. L.; Schmittel, M. *Org. Biomol. Chem.* **2012**, *10*, 4651.

(7) (a) Lehn, J.-M.; Eliseev, A. V. *Science* **2001**, *291*, 2331. (b) Northrop, B. H.; Yang, H.-B.; Stang, P. J. *Inorg. Chem.* **2008**, *47*, 11257. (c) Zheng, Y.-R.; Yang, H.-B.; Northrop, B. H.; Ghosh, K.; Stang, P. J. *Inorg. Chem.* **2008**, *47*, 4706. (d) Zheng, Y.-R.; Northrop, B. H.; Yang, H.-B.; Zhao, L.; Stang, P. J. *J. Org. Chem.* **2009**, *74*, 3554. (e) Zheng, Y.-R.; Yang, H.-B.; Ghosh, K.; Zhao, L.; Stang, P. J. *Chem.—Eur. J.* **2009**, *15*, 7203.

(8) (a) Sun, S.-S.; Anspach, J. A.; Lees, A. J. *Inorg. Chem.* **2002**, *41*, 1862. (b) Heo, J.; Jeon, Y.-M.; Mirkin, C. A. *J. Am. Chem. Soc.* **2007**, *129*, 7712. (c) Dublin, S. N.; Conticello, V. P. *J. Am. Chem. Soc.* **2008**, *130*, 49.

(9) Sun, S.-S.; Stern, C. L.; Nguyen, S. T.; Hupp, J. T. *J. Am. Chem. Soc.* **2004**, *126*, 6314.

(10) Zhao, L.; Northrop, B. H.; Stang, P. J. *J. Am. Chem. Soc.* **2008**, *130*, 11886.

(11) Abourahma, H.; Moulton, B.; Kravtsov, V.; Zaworotko, M. J. *J. Am. Chem. Soc.* **2002**, *124*, 9990.

(12) Halper, S. R.; Cohen, S. M. *Angew. Chem., Int. Ed.* **2004**, *43*, 2385.

(13) (a) Tashiro, S.; Kobayashi, M.; Fujita, M. *J. Am. Chem. Soc.* **2006**, *128*, 9280. (b) Suzuki, K.; Kawano, M.; Sato, S.; Fujita, M. *J. Am. Chem. Soc.* **2007**, *129*, 10652. (c) Ferrer, M.; Gutiérrez, A.; Mounir, M.; Rossell, O.; Ruiz, E.; Rang, A.; Engeser, M. *Inorg. Chem.* **2007**, *46*, 3395. (d) Yamauchi, Y.; Yoshizawa, M.; Fujita, M. *J. Am. Chem. Soc.* **2008**, *130*, 5832. (e) Rang, A.; Engeser, M.; Maier, M. M.; Nieger, M.; Lindner, W.; Schalley, C. A. *Chem.—Eur. J.* **2008**, *14*, 3855. (f) Ono, K.; Klosterman, J. K.; Yoshizawa, M.; Sekiguchi, K.; Tahara, T.; Fujita, M. *J. Am. Chem. Soc.* **2009**, *131*, 12526. (g) Ferrer, M.; Gutiérrez, A.; Rodríguez, L.; Rossell, O.; Ruiz, E.; Engeser, M.; Lorenz, Y.; Schilling, R.; Gómez-Sahl, P.; Martín, A. *Organometallics* **2012**, *31*, 1533.

(14) (a) Yuan, Q.-H.; Yan, C.-J.; Yan, H.-J.; Wan, L.-J.; Northrop, B. H.; Jude, H.; Stang, P. J. *J. Am. Chem. Soc.* **2008**, *130*, 8878. (b) Rang, A.; Nieger, M.; Engeser, M.; Lützen, A.; Schalley, C. A. *Chem. Commun.* **2008**, 4789. (c) Zhao, Z.; Zheng, Y.-R.; Wang, M.; Pollock, J. B.; Stang, P. J. *Inorg. Chem.* **2010**, *49*, 8653. (d) Zheng, Y. R.; Zhao, Z.; Wang, M.; Ghosh, K.; Pollock, J. B.; Cook, T. R.; Stang, P. J. *J. Am. Chem. Soc.* **2010**, *132*, 16873. (e) Wang, M.; Vajpayee, V.; Shanmugaraju, S.; Zheng, Y. R.; Zhao, Z.; Kim, H.; Mukherjee, P. S.; Chi, K.-W.; Stang, P. J. *Inorg. Chem.* **2011**, *50*, 1506.

(15) Schmittel, M.; He, B.; Fan, J.; Bats, J. W.; Engeser, M.; Schlosser, M.; Deiseroth, H. J. *Inorg. Chem.* **2009**, *48*, 8192.

(16) (a) Samanta, S. K.; Samanta, D.; Bats, J. W.; Schmittel, M. *J. Org. Chem.* **2011**, *76*, 7466. (b) We now use the name HETPYP-II for assemblies as reported in ref 15.

(17) (a) Schmittel, M.; Lüning, U.; Meder, M.; Ganz, A.; Michel, C.; Herderich, M. *Heterocycl. Commun.* **1997**, *3*, 493. (b) Schmittel, M.; Kalsani, V.; Bats, J. W. *Inorg. Chem.* **2005**, *44*, 4115. (c) De, S.; Mahata, K.; Schmittel, M. *Chem. Soc. Rev.* **2010**, *39*, 1555.

(18) (a) Schmittel, M.; Ganz, A.; Fenske, D. *Org. Lett.* **2002**, *4*, 2289. (b) Schmittel, M.; Ammon, H.; Kalsani, V.; Wiegrefe, A.; Michel, C. *Chem. Commun.* **2002**, 2566. (c) Schmittel, M.; Kalsani, V.; Fenske, D.; Wiegrefe, A. *Chem. Commun.* **2004**, 490. (d) Schmittel, M.; Kishore, R. S. K. *Org. Lett.* **2004**, *6*, 1923. (e) Kishore, R. S. K.; Paululat, T.; Schmittel, M. *Chem.—Eur. J.* **2006**, *12*, 8136. (f) Schmittel, M.; Kishore, R. S. K.; Bats, J. W. *Org. Biomol. Chem.* **2007**, *5*, 78. (g) Fan, J.; Bats, J. W.; Schmittel, M. *Inorg. Chem.* **2009**, *48*, 6338. (h) Schmittel, M.; Mahata, K. *Chem. Commun.* **2010**, *46*, 4163.

(19) (a) Schmittel, M.; Kalsani, V.; Mal, P.; Bats, J. W. *Inorg. Chem.* **2006**, *45*, 6370. (b) Schmittel, M.; Kalsani, V.; Michel, C.; Mal, P.; Ammon, H.; Jäckel, F.; Rabe, J. P. *Chem.—Eur. J.* **2007**, *13*, 6223. (c) Schmittel, M.; He, B.; Kalsani, V.; Bats., J. W. *Org. Biomol. Chem.*

2007, *5*, 2395. (d) Schmittel, M.; Mal, P. *Chem. Commun.* **2008**, 960. (e) Schmittel, M.; He, B.; Mal, P. *Org. Lett.* **2008**, *10*, 2513.
(20) (a) Schmittel, M.; Ganz, A. *Chem. Commun.* **1997**, 999. (b) Holliday, B. J.; Mirkin, C. A. *Angew. Chem., Int. Ed.* **2001**, *40*, 2022. (c) Yamanaka, M.; Yamada, Y.; Sei, Y.; Yamaguchi, K.; Kobayashi, K. *J. Am. Chem. Soc.* **2006**, *128*, 1531. (d) Weilandt, T.; Troff, R. W.; Saxell, H.; Rissanen, K.; Schalley, C. A. *Inorg. Chem.* **2008**, *47*, 7588 The combination of several bi- or tridentate ligands at dynamically binding metal centers in supramolecular assemblies operates at the cost of a slow kinetics and thus would not be ideal for a model study on the interconversion of supramolecules..
(21) (a) Fujita, M.; Oguro, D.; Miyazawa, M.; Oka, H.; Yamaguchi, K.; Ogura, K. *Nature* **1995**, *378*, 469. (b) Olenyuk, B.; Whiteford, J. A.; Fechtenkötter, A.; Stang, P. J. *Nature* **1999**, *398*, 796. (c) Yoshizawa, M.; Nakagawa, J.; Kumazawa, K.; Nagao, M.; Kawano, M.; Ozeki, T.; Fujita, M. *Angew. Chem., Int. Ed.* **2005**, *44*, 1810. (d) Fujita, M.; Tominaga, M.; Hori, A.; Therrien, B. *Acc. Chem. Res.* **2005**, *38*, 371. (e) Sato, S.; Lida, J.; Suzuki, K.; Kawano, M.; Ozeki, T.; Fujita, M. *Science* **2006**, *313*, 1273.
(22) Yoshizawa, M.; Nagao, M.; Kumazawa, K.; Fujita, M. *J. Organomet. Chem.* **2005**, *690*, 5383.
(23) Lopez, S.; Keller, S. W. *Inorg. Chem.* **1999**, *38*, 1883.
(24) (a) Schmittel, M.; Kalsani, V.; Kishore, R. S. K.; Cölfen, H.; Bats, J. W. *J. Am. Chem. Soc.* **2005**, *127*, 11544. (b) Schmittel, M.; He, B. *Chem. Commun.* **2008**, 4723. (c) Schmittel, M.; Michel, C.; Liu, S.-X.; Schildbach, D.; Fenske, D. *Eur. J. Inorg. Chem.* **2001**, 1155. (d) Ogi, S.; Ikeda, T.; Wakabayashi, R.; Shinkai, S.; Takeuchi, M. *Chem.—Eur. J.* **2010**, *16*, 8285.
(25) (a) Fujita, M.; Kwon, Y. J.; Washizu, S.; Ogura, K. *J. Am. Chem. Soc.* **1994**, *116*, 1151. (b) Blake, A. J.; Hill, S. J.; Hubberstey, P.; Li, W. S. *J. Chem. Soc., Dalton Trans.* **1997**, 913. (c) Noguchi, D.; Tanaka, H.; Kondo, A.; Kajiro, H.; Noguchi, H.; Ohba, T.; Kanoh, H.; Kaneko, K. *J. Am. Chem. Soc.* **2008**, *130*, 6367.
(26) (a) MacGillivray, L. R.; Subramanian, S.; Zaworotko, M. J. *J. Chem. Soc., Chem. Commun.* **1994**, 1325. (b) Blake, A. J.; Hill, S. J.; Hubberstey, P.; Li, W. S. *J. Chem. Soc., Dalton Trans.* **1998**, 909.
(27) (a) Lewis, D. F.; Lippard, S. J.; Welcker, P. S. *J. Am. Chem. Soc.* **1970**, *92*, 3805. (b) Kappenstein, C.; Hugel, R. P. *Inorg. Chem.* **1978**, *17*, 1945. (c) Sorrell, T. N.; Malachowski, M. R.; Jameson, D. M. *Inorg. Chem.* **1982**, *21*, 3250. (d) Munakata, M.; Maekawa, M.; Kitagawa, S.; Matsuyama, S.; Masuda, H. *Inorg. Chem.* **1989**, *28*, 4300. (e) Chou, C.-C.; Su, C.-C.; Yeh, A. *Inorg. Chem.* **2005**, *44*, 6122. (f) Chou, C.-C.; Liu, H.-J.; Chao, L. H.-C. *Chem. Commun.* **2009**, 6382.
(28) Potts, K. T.; Horwitz, C. P.; Fessak, A.; Keshavarz-K, M.; Nash, K. E.; Toscano, P. J. *J. Am. Chem. Soc.* **1993**, *115*, 10444.
(29) *SAINT*, version 6.02; Bruker AXS: Madison, WI, 1999.
(30) Sheldrick, G. M. *SHELXS-97 and SHELXL-97: Program for the Crystal Structure Solution and Refinement*; University of Göttingen: Göottingen, Germany, 1997.
(31) Sheldrick, G. M. *SHELXTL Reference Manual*, version 5.1; Bruker AXS: Madison, WI, 1997.